Maghemite in Icelandic basalts

S. STEINTHORSSON AND Ö. HELGASON
Science Institute, University of Iceland, Dunhagi 3, IS-107, Reykjavík, Iceland
M. B. MADSEN
Physics Laboratory, H.C. Ørstedt Institute, DK-2100 Copenhagen Ø, Denmark
C. BENDER KOCH, M. D. BENTZON AND S. MØRUP
Laboratory of Applied Physics, Technical University of Denmark, DK-2800, Lyngby, Denmark

Abstract

Curie temperatures indicating non-titaniferous magnetite are common in Icelandic basalts of all ages, especially Tertiary ones. Yet, microprobe analyses of such samples have shown high titanium in the magnetite. To resolve this paradox, and the mechanism at work, the magnetic mineral fraction of eight basalt samples with J_s–T curves characteristic for pure magnetite was subjected to a multi-disciplinary analysis including Mössbauer spectroscopy and X-ray diffraction. In most of the samples titanium in the magnetite, as analysed with the microprobe, ranged between 16 and 28 wt.%, indicating submicroscopic solvus exsolution in the titanomagnetite, beyond the power of resolution for the microprobe. More unexpectedly in view of the reversible J_s–T curves, Mössbauer spectroscopy showed appreciable proportion of maghemite in the magnetic fraction. A three-stage mechanism is proposed for the formation of the mineral assemblages observed: (1) limited high-temperature oxyexsolution; (2) solvus exsolution during low-temperature hydrothermal alteration; and (3) maghemitization of the magnetite. Finally, the maghemite may transform to hematite with time. It is concluded that maghemite is much more common in Icelandic rocks than hitherto believed.

KEYWORDS: maghemite, basalts, Mössbauer spectroscopy, X-ray diffraction, Iceland.

Introduction

THE oxidation of titanomagnetite ($Fe_{3-x}Ti_xO_4$, $0 \leqslant x \leqslant 1$) to titanomaghemite ($\gamma$-$Fe_{(3-x)R}Ti_{xR}\square_{3(1-R)}O_4$, where $\square$ = vacancies and R varies from 1 (stoichiometric) to $R = 8/(3 + x)$) (O'Reilly, 1984) has received increased attention in recent years following Irving's (1970) suggestion that the ubiquitous decrease in palaeomagnetic intensities away from the mid-ocean ridges results from this process (Smith, 1987). In subaerial basalts a few occurrences of titanomaghemite have also been described (Akimoto and Kushiro, 1960; Imsland, 1984), in addition to the well-known formation of maghemite (γ-Fe_2O_3) as a surface weathering product of basalts (Allan *et al.*, 1988; Mørup *et al.*, 1990). Here we report a study on subaerial basalts from Iceland indicating an overall process in which titanomagnetite is transformed into pure (non-titaniferous) maghemite in three stages, involving, first, limited oxyexsolution at magmatic and deuteric temperatures, second, solvus exsolution due to hydrothermal alteration and, third, oxidation of the magnetite to maghemite.

The Mössbauer technique offers an excellent method for determining the iron oxides in rocks, including the more elusive ones like maghemite. A multi-disciplinary reconnaissance study was made of the oxide minerals from eight samples of basaltic lava from Iceland, ranging in geological age from 40000 yrs to 15 m.y. The study grew out of our earlier investigations on highly magnetic basalts from the Stardalur caldera (Helgason *et al.*, 1990), in which the samples showed characteristically high single Curie temperature and reversible J_s–T curve (Fig. 1). In continuation of that study, the present samples were selected on the basis of their similar thermomagnetic behaviour. Especially the reversibility of the J_s–T curve of the present samples we found rather surprising in view of the fact that the Mössbauer study indicates appreciable amount of maghemite in six out of the eight samples, between 16 and

Mineralogical Magazine, June 1992, Vol. 56, pp. 185–199

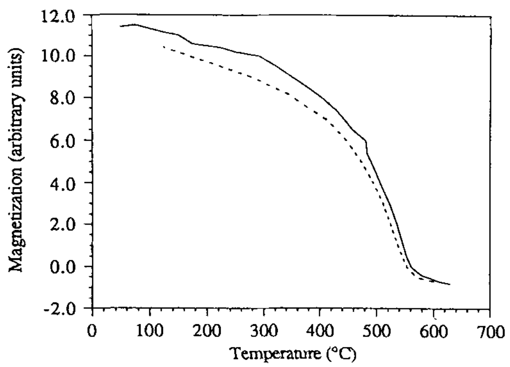

FIG. 1. Magnetisation curve for sample LY-7, representative for all the samples, showing high degree of reversibility and Curie temperature of approx. 580 °C.

60% of the magnetic phase. High Curie temperatures are common in Icelandic lavas of all geological ages, and in Tertiary lavas almost exclusively so (Becker, 1980); the question therefore arises as to what role maghemite plays in the mineralogical evolution and magnetic properties of these rocks.

According to Ade-Hall *et al.* (1971), J_s-T curves with a high single Curie temperature (Fig. 1) are characteristic of either a high degree of deuteric oxidation or advanced hydrothermal alteration of Ti-rich titanomagnetite. In our work, instances of both types (but with no maghemite present) have been encountered. A combination of X-ray diffraction (XRD), microprobe, and Mössbauer analyses indicated that in both cases the pure magnetite was formed by subsolvus exsolution in the titanomagnetite. Instances of pure magnetite formed by deuteric oxidation are characteristically found in gabbros (unpublished results), whereas the most pristine example of exsolution due to post-crystallisation reheating was found in the aforementioned lavas filling the Stardalur caldera (Steinthorsson and Sigvaldson, 1971; Steinthorsson *et al.*, 1971; Fridleifsson and Kristjansson, 1972). Relative to the Stardalur suite, the present samples, although exhibiting high Curie temperatures and similar J_s-T curves, possess weaker remanent magnetisation and more heterogeneous mineralogy.

Samples

The eight samples studied (Fig. 2, Table 1 and Appendix) were in the form of 1" drill cores from the collection of Dr. Leo Kristjansson. The samples marked LX, LY and WJ are examples of series of drill cores taken in a horizontal progression out from dykes traversing the Plio-Pleistocene lava succession near Reykjavik, to investigate the effects of alteration resulting from the intrusion (Kristjansson, 1985). The sample HV-10 is from a geomagnetic excursion near Reykjavik (Levi *et al.*, 1990). The remaining samples, although coming from different parts of the country, represent a progression in age and degree of hydrothermal alteration, as indicated by the zeolite assemblage of the rock (Kristjansson, 1985).

Walker (1960) mapped subhorizontal zones of zeolite assemblages in eastern Iceland which are related to the maximum temperature experienced by the rock during burial and alteration (Oskarsson *et al.*, 1982). The relevant temperatures for the present samples are in the order of 70, 85 and 100 °C for the chabazite, analcime and mesolite zones, respectively, based on measurements in drill holes (Steinthorsson *et al.*, 1987). Again, these zones correspond approximately to A, B and C–D in Fig. 1 of Ade-Hall *et al.* (1971). Descriptions of the samples are summarized in Table 1 and Appendix.

Methods of investigation and experimental results

Sample preparation. The samples were crushed in a jaw crusher and polished mounts made of a few pieces for optical investigation and analysis with the electron microprobe. The remainder was ground and the magnetic fraction was separated with a hand magnet, repeatedly grinding the separate to finer and finer grain size so as to obtain as pure a fraction as possible. In addition, some of the samples were separated in heavy liquids to obtain the undifferentiated heavy mineral fraction. Mössbauer spectra were obtained of both the magnetic fraction and the bulk sample. In preparation for the X-ray and Mössbauer analyses the samples were ground by hand under acetone in an agate mortar.

X-ray diffraction. The samples were analysed with X-ray diffraction, using Cu-$K\alpha$ radiation filtered with Ni. The spectrometer ran between 31 and 36°, to include the NaCl peak (internal standard) at 31.69° and the (311) diffraction peak for magnetite (and maghemite); this 2θ range also includes peaks for olivine, ilmenite, and augite. For titanomagnetite the 2θ value of the (311) peak varies from 35.43° for pure magnetite (Mt_{100}) to 34.99° for $Mt_{30}Usp_{70}$, corresponding to unit-cells of 8.396 and 8.497 Å, respectively (Fig. L-6 in Lindsley, 1976*a*). The corresponding unit-cell for pure maghemite is 8.34 Å. For nonstoichiometric, non-titaniferous magnetite the unit-cell varies continuously between pure magnetite and maghemite (Fig. L-9 in Lindsley, 1976*a*).

Table 2 lists the unit-cell (a_o) calculated from the X-ray diffractograms, together with the ratio Mh/(Mh + Mt) as determined with Mössbauer analysis (Table 1). In all instances a single, somewhat broadened X-ray peak was obtained that could not be resolved into two, even at the highest resolution attainable with the instrument. The calculated cell edge values tend to be on the 'maghemite side' of pure magnetite, and generally there is a fair agreement between the position of the X-ray peak and the percentage of maghemite as determined by Mössbauer spectroscopy (Table 2, columns 2 and 3). However, the XRD-analysis does not, *per se*, resolve whether the peak is due to nonstoichiometric magnetite or a mixture of maghemite and magnetite—for that to be determined, Mössbauer spectroscopy was required. Among the oxidised samples, HV-10 and JGC-7 are exceptions in having unit-cell edges larger than 8.396 Å (pure magnetite), indicative either of titanomagnetite (col. 4) or titanomaghemite.

Of interest, too, is the fact that despite the separation technique described above, the magnetite could not in some of the samples be isolated from the accompanying ilmenite owing to their extremely fine intergrowth. Column 5 in Table 2 gives the height of the ilmenite (104) peak, in (%), relative to that of magnetite in the diffractogram.

In the Table, three young lava flows are included for comparison, showing the expected range of titanomagnetite compositions in the flows prior to hydrothermal alteration. Sample SNS-23 has one well-defined peak, SNS-8 has a main peak corresponding to Usp_{50} and an auxiliary one corresponding to Usp_{40}, whereas B-THO shows continuous zonation with decreasing intensity from Usp_{45} towards magnetite-rich compositions.

Optical mineralogy. The opaque mineral assemblages in the samples were classified optically according to the scheme described by Haggerty (1976) (Table 1 and Appendix) in which the oxidation of the spinel phase is divided into seven stages, termed C1 to C7 ('C' for cubic, see Fig. 3). A magnetite colloid (Elmore, 1938) was used to distinguish between magnetic and non-magnetic phases (Figs. 3 and 4). Relevant to the present samples, stage C1 denotes optically

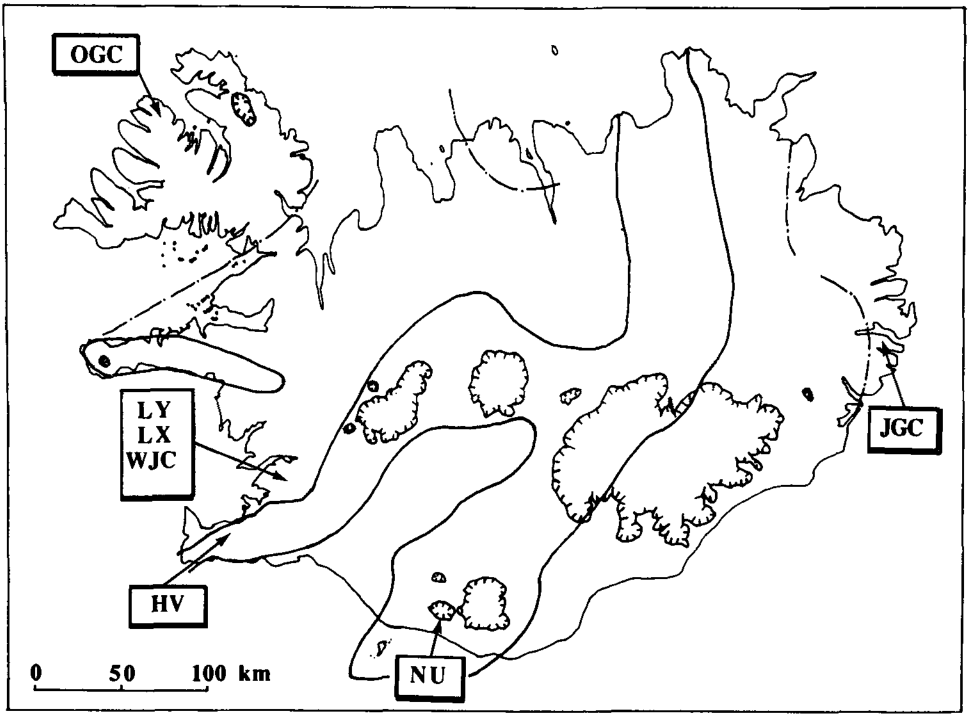

FIG. 2. Map of Iceland showing the sample localities. The Neovolcanic zones (younger than 0.7 Ma) are enclosed by full-drawn curves, and 10 Ma isochrones in the Tertiary succession (anomaly 5) are indicated by dash-dot curves. Irregular patches with patterned rims are glaciers (see Kristjansson, 1985; Levi *et al.*, 1990).

Table 1 Description of the samples. % Mt and % Mh refer to the proportion of magnetite and maghemite in the magnetic separate, as determined from the fit of the Mössbauer spectra. Oxidation stage (Ox, stage) is optically determined according to Haggerty (1976)

Sample	Age (Ma)	Zeolite zone	% Mt	% Mh	Ox stage	Grain size of magnetite
HV-10	0.04	no zeol$^{1)}$	45	20	C1	<0.02mm
NU-12-1	0.7	no zeol$^{1)}$	38	18	C3,C7	0.013mm
LX-2	2	analcime$^{2)}$	54	10	C1	0.2x0.02mm^2
LX-6	2	analcime$^{2)}$	56	12	C3,C7	<0.08x0.06mm^2
LY-7	2	analcime$^{2)}$	30	30	C2	<0.8x0.6mm^2
WJC-6	2	analcime /mesolite$^{2)}$	30	30	C1	<0.1mm
JGC-7	10	mesolite$^{2,3)}$	65	0	C2	<0.16x0.12mm^2
OGC-1	15	chabazite$^{2)}$	65	0	C2,C7	<0.1mm

References refer to orginal descriptions of the samples:
$^{1)}$ Levi et al. (1990)
$^{2)}$ Kristjansson (1985)
$^{3)}$ Helgason (1982)

homogeneous titaniferous magnetite, stage C2 the presence of small amount of exsolved ilmenite lamellae parallel to the {111} planes of the cubic host, and stage C3 magnetite grains crowded with exsolution lamellae. Stage C7 is characterised by the assemblage pseudobrookite + hematite. As seen in Table 1, the oxidation stage is quite variable within some of the samples, presumably reflecting the parameters such as distance from the surface of the lava flow or some local influence of volatiles.

As shown by the microprobe analyses in Table 3, the magnetite (spinel) in most of the samples contains considerable amount of TiO_2. Despite this, other analyses (X-ray, Curie-temperature and Mössbauer spectroscopy) show that the spinel phase in all eight samples is almost non-titaniferous. Therefore, the opaque mineralogy must reflect two phases of oxidation and alteration, termed primary and secondary. In the primary, high-temperature or deuteric stage, oxyexsolution up to stage C3 probably took place during closed-system cooling in the lava flow, leading in stage C3 to quite Ti-poor spinel (e.g. NU-12 and OGC-1, Table 3 and Fig. 3*c*). Conversely, primary oxidation to the highest stages (C7, Fig. 3*d*) reflects open-system cooling, i.e. one in which oxidation was influenced either by atmospheric contamination or degassing of the crystallising lava (Sato and Wright, 1966); such oxidation can also cause exsolution of either hematite or magnetite from olivine (Haggerty and

Table 2: Compositions of magnetic minerals in some samples, as determined by X-ray diffraction (XRD) and Mössbauer spectroscopy (MS)

	XRD a_o (Å)	MS Mh (%)	XRD Mh (%)	XRD Usp (%)	XRD Im (%)
HV-10	8.40	31	0	04	18
NU-12	n.d.	32	n.d.	n.d.	n.d.
LX-2	8.39	16	20	-	0
LX-6	8.39	18	20	-	14
LY-7	8.38	50	40	-	0
WJC-6	8.38	50	40	-	23
JGC-7	8.405	0	(0)	10	32
OGC-1	n.d.	0	n.d.	n.d.	n.d.
B-THO	8.46	n.d.	-	45 (35-06)	0
SNS-8	8.47	n.d.	-	50 (40)	0
SNS-23	8.50	n.d.	-	70	0

n.d.: not determined
- : doesn't apply

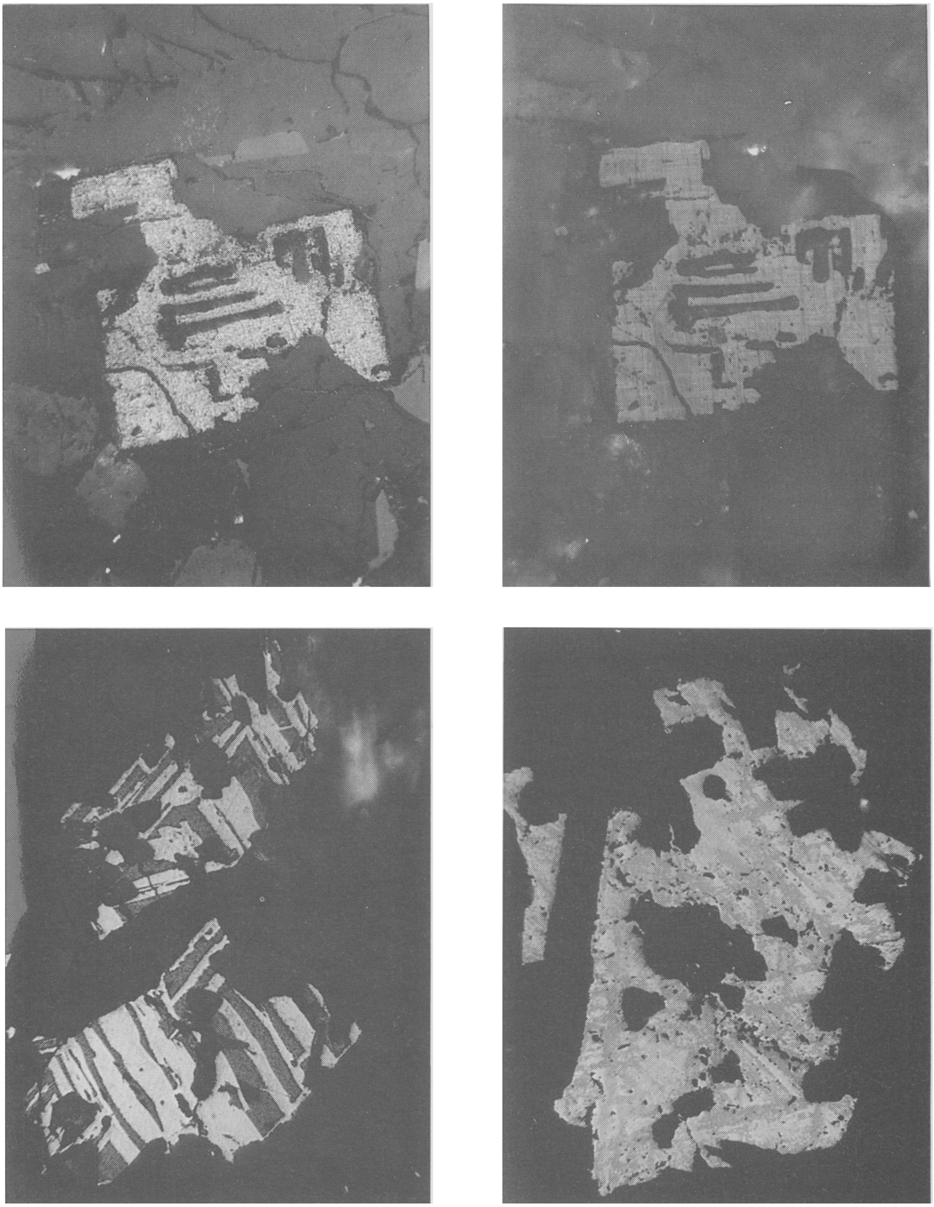

FIG. 3(*a*,*b*). Homogeneous titanomagnetite (stage C1). The magnetite, as indicated by the magnetic colloid in (*a*, *upper left*), appears optically anisotropic under crossed nicols (*b*, *upper right*) owing to submicroscopic exsolution lamellae of ilmenite and hematite. Sample JGC-7. Reflected light, length of field 0.3 mm. (*c*, *lower left*) Titanomagnetite oxidised to stage C3, with magnetite colloid bringing out sandwich pattern of ilmeno-hematite exsolution lamellae. Sample OGC-1. Plane-polarised reflected light, length of field 0.3 mm. (*d*, *lower right*) Titanomagnetite oxidised to stage C7, consisting of pseudobrookite and hematite. Sample OGC-1. Plane polarised reflected light, length of field 0.3 mm.

Baker, 1967), as seen in some of the samples (Appendix). One case of high-temperature oxidation is summarised in Fig. 5A.

Secondary, low-temperature alteration took place during regional hydrothermal reheating of the lava pile and resulted in solvus exsolution of titanomagnetite to form nearly pure magnetite and an ulvöspinel-rich phase (Figs. 3*a* and 4*a*). Owing to the skewness of the solvus, all compositions of the titanomagnetite solid solution exsolve to form nearly pure magnetite below approx. 500 °C (Basta, 1960). Part of the magnetite was subsequently oxidised to maghemite (Fig. 4*b*) and, eventually in some of the samples, to hematite, whereas the Usp-rich part invariably oxidises to a hematite-ilmenite assemblage (Fig. 5B) as dictated by the presence of a solvus in the system $FeTiO_3$–α-Fe_2O_3 (Carmichael, 1961).

In some of the samples the magnetite colloid showed the titanomagnetite grains to be entirely magnetic (C1 stage), with no octahedral exsolution lamellae of ilmenite (Fig. 3*a*). With crossed nicols, however, these grains are anisotropic, exhibiting in some cases apparently lamellar extinction pattern (Fig. 3*b*). The tartan extinction pattern in Fig. 3*b* is considered to be parallel to the cube faces {100} in the magnetite. Similar phenomena have been described in an oxidised basalt (e.g. Watkins and Haggerty, 1967), and in dykes in which, however, the extinction was patchy rather than lamellar (Jensen, 1968). In both instances, since the microprobe analyses show considerable Ti in magnetite that according to XRD and Mössbauer spectroscopy is non-titaniferous, the explanation must be solvus exsolution of the Mt_{ss} to form a sub-microscopic intergrowth (cloth texture of Ramdohr, 1953).

Table 3 shows representative microprobe analyses of the oxides in the eight samples. The columns labelled 'Im' are primary high-temperature hemo-ilmenite, the ones labelled 'Mt' are titanomagnetite having undergone low-temperature solvus exsolution. The analyses were recalculated into end-member compositions according to the scheme of Carmichael (1967). Since the 'Mt' analyses in fact express a sub-microscopic assemblage of magnetite + ilmenite + hematite in variable proportions, these analyses were recalculated both as Mt_{ss} and Im_{ss}, giving in most cases low totals for the former Mt_{ss} and high for the latter Im_{ss}. Ideally, were the analyses completely accurate, and included all elements present, the relative proportions of the three minerals could be calculated from the analyses

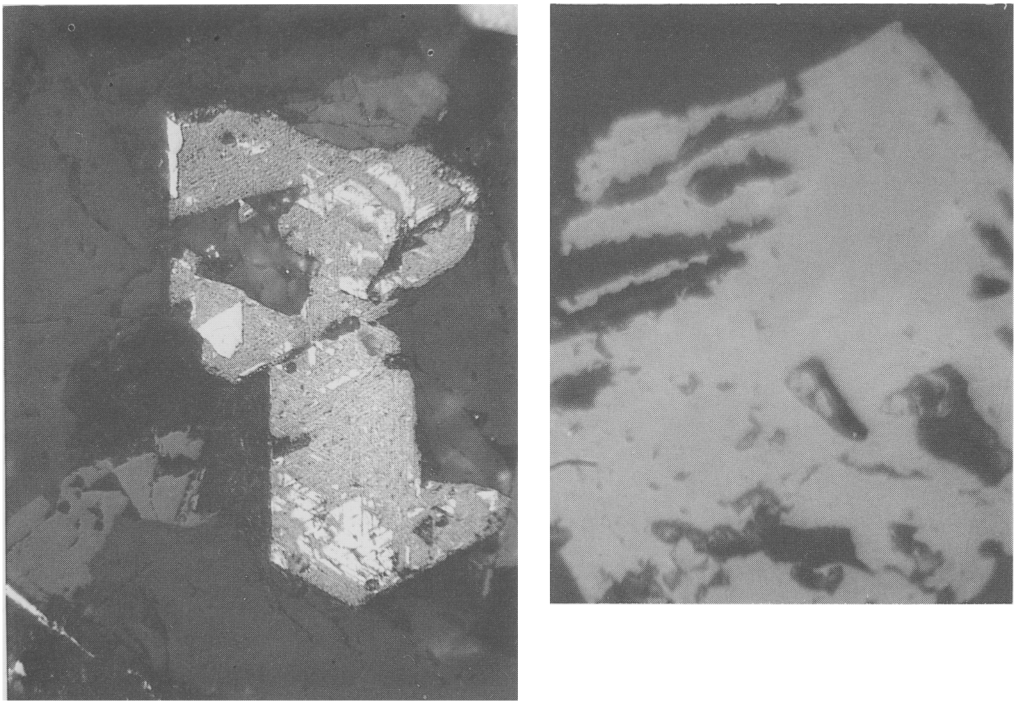

FIG. 4 (*a, left*) Crystal exhibiting parallel growth of ilmenite (white) and titanomagnetite (stage C1, dark colour due to magnetite colloid), in which the latter has undergone secondary solvus-exsolution. Sample JGC-7. Plane polarised reflected light, magnetite colloid, length of field 0.3 mm. (*b, right*) Skeletal titanomagnetite half replaced by maghemite (light). Under the ore microscope the magnetite appears tan-coloured with a pinkish hue, the maghemite is of bluish-white colour. Sample WJC-6. Plane polarized reflected light, length of field 0.1 mm.

Table 3: Representative microprobe analyses of opaques from the eight samples. The analyses are recalculated according to Carmichael (1967), those of the spinel phase (Mt) both into rhombohedral and spinel end members (see the text). The range of TiO_2 values in exsolved titanomagnetite, together with the number of points analyzed, is given at the bottom.

	LX-6		LY-7		LX-2	JGC		OGC-1		WJC-6		NU-12	HV-10	
	Im	Mt	Im	Mt	Mt	Im	Mt	Im	Mt	Im	Mt	Mt	Im	Mt
CaO	n.d	n.d.	n.d.	n.d.	n.d.	n.d.	n.d.	0,4	n.d.	n.d.	n.d.	n.d.	n.d.	n.d.
Al_2O_3	1,1	2,0	0,9	2,9	2,0	0,2	2,0	0,0	3,2	0,1	2,1	1,2	n.d.	2,0
FeO	54,5	67,0	47,4	66,1	65,1	48,6	64,8	49,8	86,9	47,3	63,8	86,2	45,5	77,2
TiO_2	41,1	27,5	44,2	26,1	26,2	48,3	26,7	43,8	4,9	50,0	27,6	6,0	49,2	15,5
SiO_2	n.d.	n..d.	n.d.	n.d.	n.d.	n.d.	n.d.	0,9	n.d.	n.d.	n.d.	n.d.	n.d.	n.d.
MgO	0,7	0,7	2,0	0,9	0,4	0,9	0,9	2,3	1,1	1,0	0,1	1,0	2,7	1,1
MnO	0,3	0,7	0,7	0,5	1,3	0,9	3,4	0,8	0,3	0,9	4,2	0,5	n.d.	n.d.
Total	97,6	97,9	95,3	96,5	95,0	99,0	97,8	98,0	96,4	99,2	97,8	94,9	97,4	95,8
FeO		53,5		51,1	51,2		49,8		32,6		50,9	34,1		42,5
Fe_2O_3		13,5		14,3	13,8		15,2		57,8		12,7	56,9		37,0
Total		97,8		95,9	95,0		97,9		99,9		97,5	99,8		98,1
Usp %		79,7		77,6	78,3		75,8		11,3		79,8	14,2		43,7
FeO	35,4	22,8	35,4	21,2	21,5	40,8	18,9	35,2	2,2	42,3	20,4	3,1	39,5	12,0
Fe_2O_3	21,2	49,2	13,4	49,8	48,5	8,6	51,0	16,2	94,1	5,6	48,2	92,4	6,7	72,5
Total	99,7	102,8	96,6	101,5	99,8	99,8	102,9	99,6	105,8	99,8	102,6	104,2	98,0	103,1
Hm %	21,2	48,0	13,8	50,0	48,9	8,4	49,7	15,3	90,7	5,3	47,5	88,6	6,4	70,6
TiO_2-range		35,7-		32,7-	26,3-		28,1-				30.7-	6-		18.8-
in Mt		16,6		25,7	24		23				27.6	0.7		15.5
no. of points		9		7	3		5		1		2	2		2

(all Ti in ilmenite, the iron distributed between ferrous and ferric to yield 100% total). However, as they stand, the main message conveyed by the 'Mt' analyses is their high TiO_2 and the fact that they represent mineral aggregates rather than monomineralic titanomagnetite.

Mössbauer spectroscopy. Fig. 6 shows the room-temperature Mössbauer spectrum of the magnetic fraction of sample LY-7 together with a spectrum of a sample from the Stardalur caldera in which the magnetic fraction consists of an almost pure magnetite (Helgason *et al.*, 1990). The central parts of the spectra, which are not resolved in Fig. 6, consist of doublets related to paramagnetic minerals, which are not of interest for this discussion. The six line patterns which characterise the magnetic minerals are very prominent in the spectra.

Pure hematite can easily be detected in spectra of this type due to the strong magnetic hyperfine field (51.7 T corresponding to a splitting between the outermost lines of the sextet of 16.1 mm/s), but no sign of hematite appears in the spectrum of LY-7. For the samples studied in the present work, however, it is important to check the Mössbauer spectra carefully for the presence of hematite. Hematite may, if it contains substitutional elements (e.g. Ti or Al) or if the crystallite size is below about 15 nm, exhibit magnetic hyperfine fields that are reduced compared to those of pure bulk hematite. Although hematite has a small quadrupole shift of 0.1 mm/s it may be confused with a maghemite component if it is present in the spectra only as a minor component, since in the cases mentioned the hyperfine fields could be quite similar to that of maghemite. To rule out the presence of hematite in our samples, spectra of the sample WJC-6 (in which the presence of hematite judged from the Mössbauer spectra was most likely to occur) were run at 5 K, both with 1.0 T magnetic field parallel to the gamma rays and without external magnetic field (see Fig. 7). With an external field of 1.0 T the second and fifth lines of the sextet almost disappear ruling out the presence of antiferromagnetic hematite in any appreciable amount. The distance between the remaining lines is almost 9.7 mm/s, corresponding to a hyperfine field of approximately 52 T. This hyperfine field is rather low for hematite (even if it is assumed that it has undergone the Morin transition) and in fact the small dips at the positions of the second and fifth line may be interpreted as canting of the spins in the ferrimagnetic minerals, e.g. maghemite (Allan *et al.*, 1989).

Having excluded the occurrence of hematite in the samples we will now focus on the Mössbauer spectra of the cubic iron oxides magnetite and maghemite.

Pure stoichiometric magnetite (Fe_3O_4) has a room-temperature Mössbauer spectrum consisting of two superimposed sextets with magnetic hyperfine fields of 49 and 46 T. The isomer shifts of the two sextets are 0.27 and 0.68 mm/s,

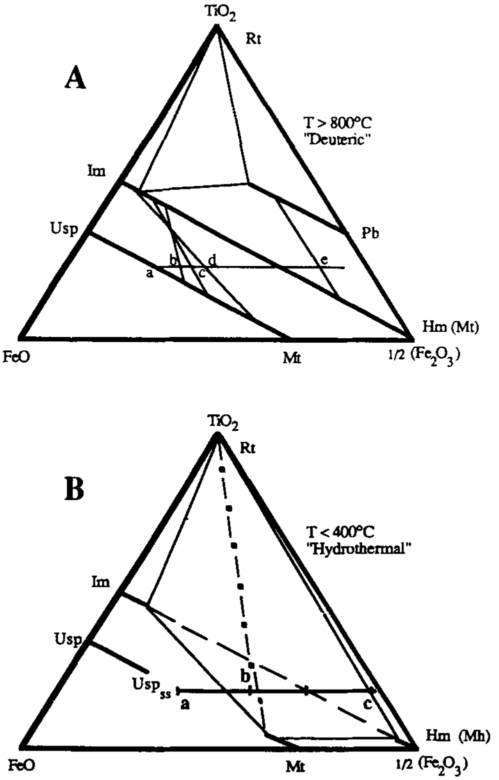

FIG. 5A. High-temperature oxidation in the system FeO–Fe_2O_3–TiO_2. Thick lines are the solid solution series ulvöspinel–magnetite (cubic spinel, Usp-Mt), ilmenite–hematite (rhombohedral, Im-Hm), and pseudobrookite (orthorhombic, Pb), respectively; thin lines indicate mineral assemblages. In the TiO_2-rich part of the system the assemblages are for 800 °C, with limited solid solution of pseudobrookite. The line *a*–*e* shows high-temperature oxidation of titanomagnetite $Mt_{30}Usp_{70}$ along the FMQ-oxygen buffer: *a*, homogeneous Mt_{SS} (stage C1); *b*, stage C2 at 1000 °C; *c*, stage C3 at 800 °C; *d*, stage C3 at 600 °C; *e*, the assemblage Hm_{SS}–Pb_{SS} (stage C7) at 800 °C. (Based on Lindsley, 1976*b*). Fig. 5B. Low-temperature oxidation in the system FeO–Fe_2O_3–TiO_3 at $T < 400$ °C. Compositions on either side of the spinel and rhombohedral miscibility gaps, respectively, are indicated schematically. The line *a*–*c* shows progressive oxidation of spinel Usp_{60} from (*a*) unmixed Usp_{SS} + Mt to (*c*) Rt + Hm (Mh). Although optically the most common assemblage in the present samples appears to be *b*: Mt + Im_{SS} (or Mt + Im + Hm—triangle including dashed line in the diagram), experimental and other evidence indicates that at low temperatures Im_{SS} + Hm_{SS} react to form Mt + Rt, as shown by the triangles including the dash-dot tie line (Lindsley, 1976*b*; Rumble, 1976). The Ti-rich phases (pseudobrookite, rutile) were not investigated specifically in the present study.

respectively, and because of the cubic surroundings of the iron atoms all quadrupole shifts are negligible. The high field sextet originates from iron in tetrahedral coordination (*A*-site) and the other from iron in octahedral coordination (*B*-site). In magnetite the occupation probabilities for the two types of sites are 0.33 and 0.67 for the two sextets corresponding to a *B*/*A*-ratios of 2/1 (Häggström *et al.*, 1978). The superposition of the two sextets with the *B*/*A*-ratio given leads to the characteristic room-temperature Mössbauer spectrum of magnetite with coinciding lines at positive velocities. The small magnetic hyperfine field and large isomer shift of the second sextet in magnetite is due to a very rapid exchange of electrons among octahedrally coordinated iron, leading to Mössbauer parameters that are averages of typical values for Fe(II) and Fe(III).

Maghemite (γ-Fe_2O_3), unlike magnetite, contains no ferrous iron and is in fact the fully oxidised counterpart of magnetite. Because of the complete oxidation of the iron in the octahedral sites in maghemite, no Fe(II) is left to participate in the rapid exchange of electrons, and as a result the Mössbauer spectrum of maghemite consists of two superimposed sextets of Fe(III) in tetrahedral and octahedral coordination. In maghemite these sextets are not resolved and only one sextet is observed in the room temperature spectrum. However, the line widths of the spectrum of maghemite show that more than one site is present in the structure. The magnetic hyperfine field of maghemite (analysed as one sextet) is 49.8 T which differs from the magnetite A-site hyperfine field by less than 1 T corresponding to a distance between the first lines of each superimposed sextet of about 0.3 mm/s. Therefore, when maghemite is present in a sample with magnetite, the high field sextet of magnetite and the sextet of maghemite cannot be resolved in the spectrum, but instead the high field sextet will appear to have a slightly larger line width. Between magnetite and maghemite a full range of intermediate phases exist; these are known as nonstoichiometric magnetites. Nonstoichiometric means that the cation/anion ratio differs from 3/4, i.e. they may be described as $Fe_{3R}\square_{(1-R)}O_4$ in which *R* is the fraction of the ideal cation/anion ratio and $\square$ is a cation vacancy. The main characteristic distinguishing Mössbauer spectra of nonstoichiometric magnetite from those of stoichiometric magnetite is a *B*/*A*-ratio lower than 2 (Ramdani *et al.*, 1987). From a comparison of the two spectra of Fig. 6 it is seen that the *B*/*A*-ratio for the sample LY-7 is quite far from the value of 2 for stoichiometric magnetite, which is applicable for the Stardalur sample shown.

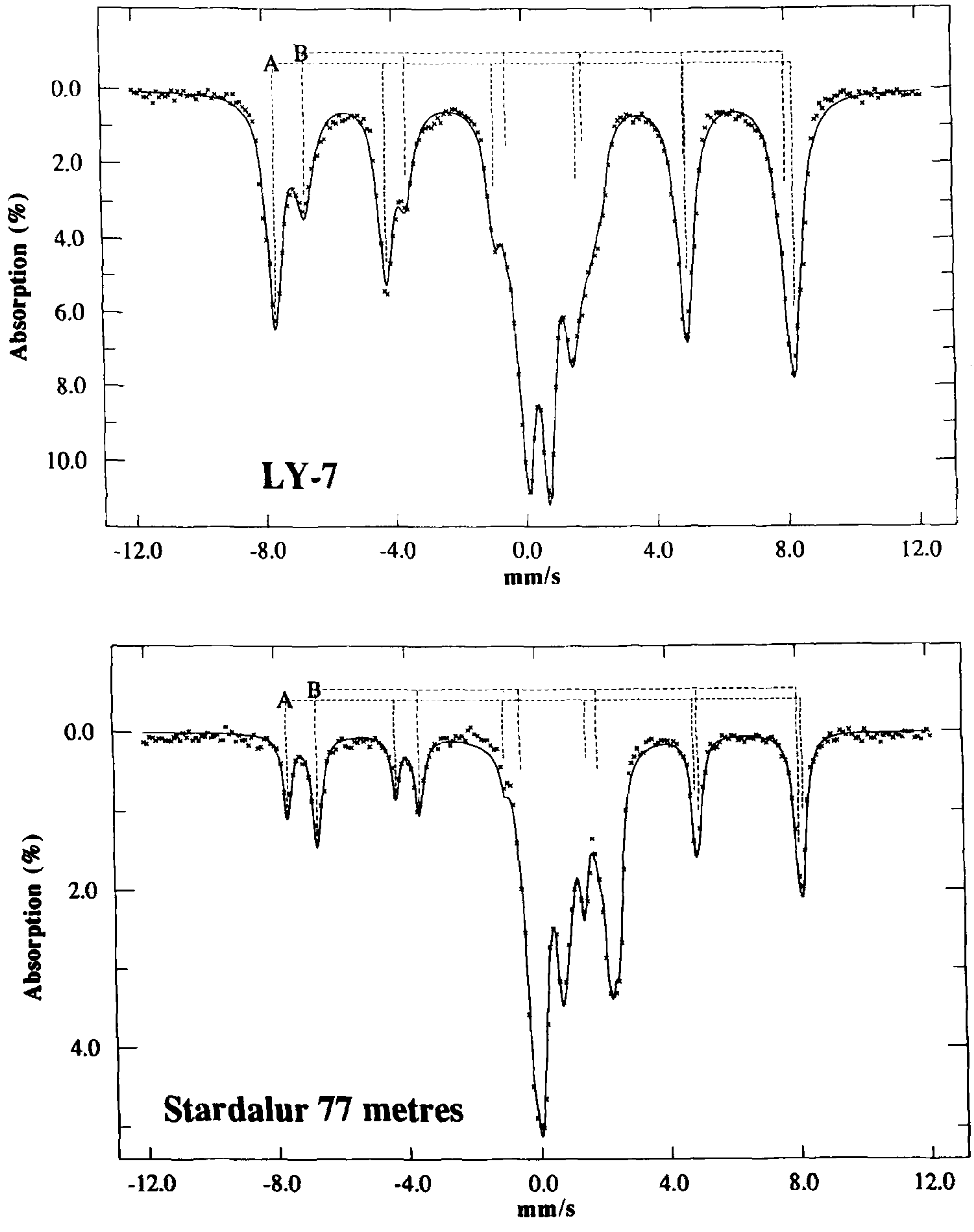

FIG. 6. Room-temperature Mössbauer spectra of sample LY-7 and a sample from the Stardalur caldera. The bar diagrams indicate the line positions of the two sextets, A and B, discussed in the text.

The ratios between the areas of the B and A sextets both for the present samples and for eight samples from Stardalur are shown in Fig. 8. It is seen that the samples can be divided into two groups. The Stardalur samples and the two Tertiary samples OGC-1 and JGC-7 all have a *B*/*A*-ratio near 2/1 indicating stoichiometric magnetite. For the other six samples this ratio is considerably smaller.

For a preliminary analysis of samples whose content of maghemite or nonstoichiometric magnetite is unknown, it is reasonable to analyse the whole spectrum in terms of two sextets, one with a hyperfine field of between 49 and 50 T and another with a field of about 46 T. Nominal occupation probabilities (*B*/*A*-ratio) are then deduced from the ratio of the spectral areas of the two sextets (assuming similar recoil-free frac-

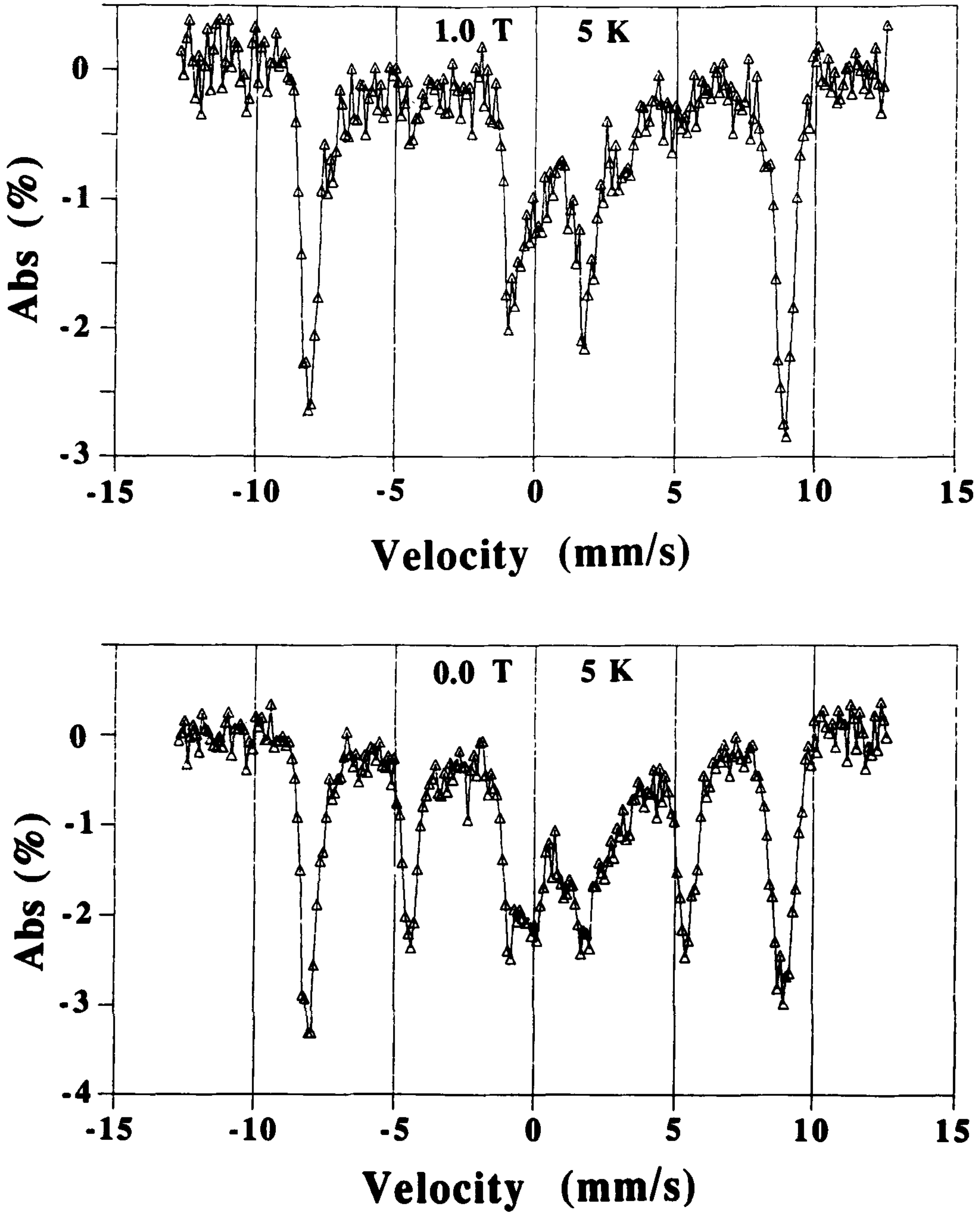

FIG. 7. Low temperature (5K) spectra of the WJC-6 sample. The lower figure shows a spectrum obtained without external magnetic field and the upper figure shows a spectrum of the sample in an external field of 1.0 Tesla perpendicular to the propagation direction of the γ-rays.

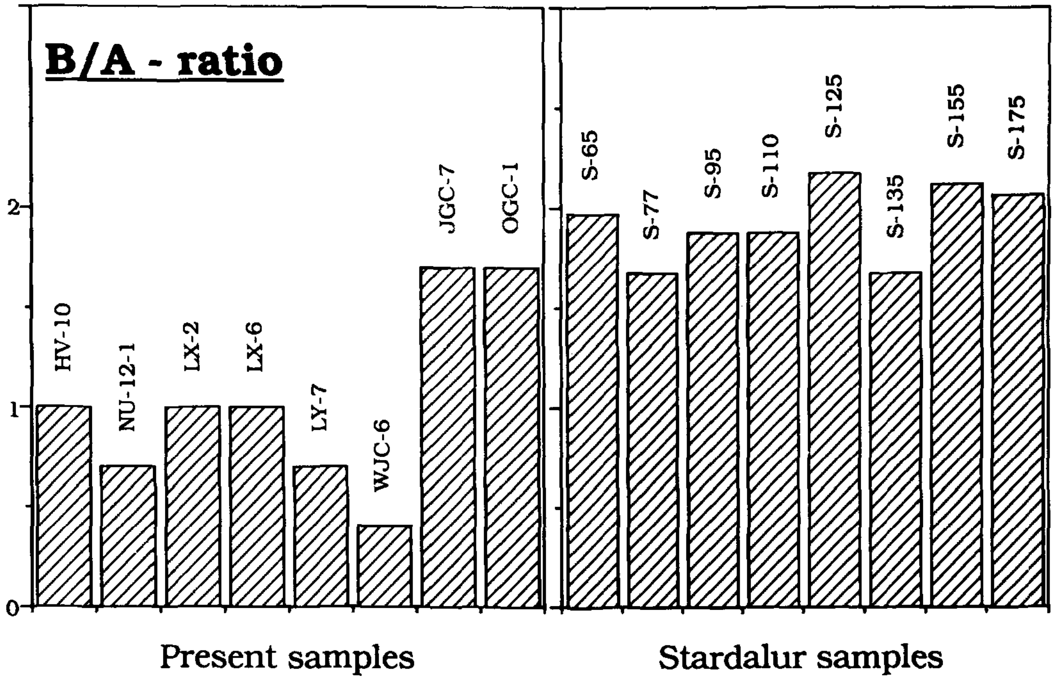

FIG. 8. The *B*/*A* ratio obtained from the Mössbauer spectra of present samples and, for comparison, eight samples from the Stardalur caldera.

tions). Deviations from the *B*/*A*-ratio of stoichiometric magnetite will then indicate either the presence of maghemite in the sample—or that the magnetite is not stoichiometric. A third possibility is that the magnetite sample contains significant amounts of a substitutional impurity (e.g. Ti). The presence of such impurities will lead to deviations from the stoichiometric *B*/*A*-ratio, but will also lead to substantial broadening of the Mössbauer lines. A comparison of the Mössbauer spectra of our samples with those of samples with known (small) amounts of Ti (Tanaka and Kono, 1987) shows that the content of Ti in our samples is well below 2%. This is also in agreement with the results from measurements of Curie temperatures. Such a low content of Ti will not affect the *B*/*A*-ratio significantly, although it may cause major changes in the Verwey transition temperature, which will be discussed in the following paragraphs.

In a homogeneous magnetite—be it stoichiometric or nonstoichiometric—there is a well defined Verwey transition temperature. This transition temperature varies continuously with the degree of non-stoichiometry from 121.5 K for a perfectly stoichiometric magnetite to about 90 K for a magnetite that has almost become maghemite (Aragon and Honig, 1988). Maghemite has no Verwey transition.

A distinction between these two possibilities (for pure iron oxides)—presence of maghemite or nonstoichiometric magnetite—may be possible by careful studies of the Verwey transition temperature(s) of the sample. If such studies show that there is a single well defined Verwey transition temperature the exact value of this is a reliable indicator of the degree of non-stoichiometry (Aragon and Honig, 1988). When the value of the non-stoichiometry is known, the distribution of spectral areas in that magnetite can be determined (Ramdani *et al.*, 1987). The difference between the *B*/*A*-ratio expected from the nonstoichiometry and the value observed experimentally can be explained by the presence of maghemite. In this way studies of the Verwey transition temperature in combination with measurements of the *B*/*A*-ratio can be used to distinguish between nonstoichiometric magnetite and mixtures of magnetite and maghemite (Madsen *et al.*, 1989). If on the other hand no definite Verwey transition temperature is found, the result of such an analysis cannot give quite as clear a conclusion about the presence of maghemite.

Studies of two of the samples close to 120 K showed that the Verwey transition temperatures for the samples are quite close to that of stoichiometric magnetite and hence it may be concluded that the magnetite in our samples is nearly stoichiometric (and does not contain significant amounts of Ti), and the low *B*/*A* ratio must therefore be due to the presence of significant amounts of maghemite. Fig. 9 shows a series of five spectra obtained at 93 K to 130 K for one of the samples.

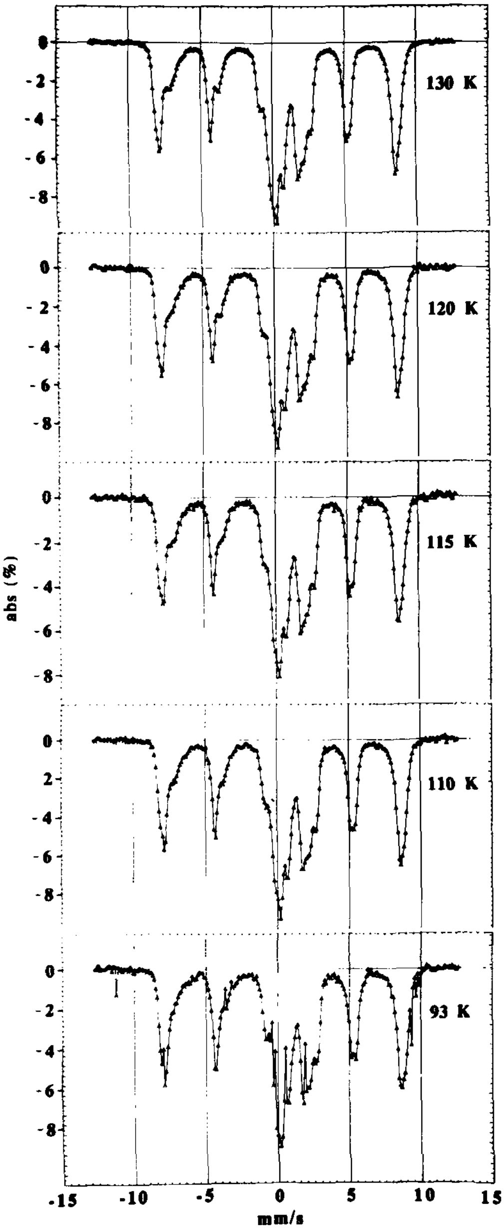

FIG. 9. A study of Verwey transition. Five spectra of the LY-sample obtained at 93 K to 130 K.

To further confirm the presence of maghemite, sample WJC-6 was subjected to electron diffraction analysis. Based on the analysis of selected area electron diffraction patterns, and from energy dispersive X-ray spectroscopy, the sample was found to contain Ti-free magnetite and maghemite (the latter exhibiting superstructure lines at 5.37, 4.32, and 3.75 Å) and Ti-containing maghemite with a Fe:Ti ratio of 3:1.

Stability of the maghemite. Due to the well known transformation of maghemite to hematite at 350 °C (O'Reilly, 1984), and the corresponding reduction in magnetisation, the presence of maghemite seems contradictory to the reversible J_s–T curves up to 580 °C. To investigate the stability of the maghemite the kinetics of the maghemite inversion was studied in sample LY-7 by heating the magnetic fraction, containing nearly equal amount of magnetite and maghemite, to 590 °C in different atmospheres and for different lengths of time (Helgason *et al.*, 1992). As expected, the amount of magnetite decreases through transformation to hematite during heating in an oxidising atmosphere (air). Considerable amount is already transformed after half an hour.

For maghemite, the results from heating the sample in an oxidising atmosphere are quite interesting. Most of the maghemite seems to withstand a few hours' heating under these conditions, at temperatures well above the 350 °C at which pure maghemite is expected to transform to hematite. The reason for this stability is not clear from this experiment. However, although the spectra indicate pure maghemite, the presence of some stabilising cations (e.g. Ti) is not precluded.

The sample treated in a reducing atmosphere shows a nearly complete transformation of both maghemite and hematite into magnetite in only 30 minutes.

These results show the importance of a careful selection of the experimental conditions for measuring the magnetisation as function of temperature. Secondly, due to the stability of maghemite (titanomaghemite) for at least the length of time usually required for J_s–T measurements (in the order of one hour), the reversibility of the J_s–T curve cannot be taken as evidence for magnetite as the sole ferrimagnetic component.

In addition, these experiments support the idea (Readman and O'Reilly, 1972) that maghemite represents an intermediate stage in the oxidation of magnetite to hematite.

Conclusions

The Mössbauer, X-ray diffraction, and electron microprobe studies give unambiguous evidence for the presence of nearly pure magnetite in all eight samples, and significant amounts of maghemite in six out of the eight samples of basalt, spanning the geological age of Iceland. The results of the present study therefore suggest that maghemite is much more common in basalts than hitherto believed. It is likely that, in these rocks, the maghemite was generally formed hydrothermally because, first, it usually doesn't occur in recent lava flows and, second, if it was present during cooling of the original lava flow it would be expected to transform to hematite. An exception is the present sample HV-10 which comes from the slaggy bottom of a picritic flow which probably was oxidized by underlying water-logged tuff. In two of the eight samples (NU-12 and OGC-1) the non-titaniferous magnetite probably formed during high-temperature oxidation to stage C3, with subsequent low-temperature oxidation to maghemite; in the others the process indicated involves sub-solvus exsolution of titanomagnetite.

In basalt samples from the ocean floor, titanomaghemite (rather than maghemite) seems to be the rule, and the scenario envisaged for the formation of the maghemitised and hematised opaque assemblages in these rocks is a two-stage one: (1) low-temperature oxidation of titanomagnetite to titanomaghemite, and (2) inversion of titanomaghemite to hematite + rutile + sphene. The process for the Icelandic subaerial, mildly hydrothermally altered basalts is somewhat more complex: titanomagnetite oxidised to stages C1–C3 is normally formed during crystallisation and cooling of lava flows. Atmospheric contamination or degassing may cause local oxidation to stage C7. Upon burial and reheating in the presence of ground water, the titanomagnetite suffers solvus exsolution at low temperatures, as indicated by the associated zeolite assemblage, to magnetite and ulvöspinel-rich titanomagnetite. The latter is quickly oxidised to ilmenite and hematite (or maghemite), whereas the oxidation of the magnetite to maghemite is less complete and probably slower. This entire process takes place in geologically short time within the volcanic zones (Oskarsson *et al.*, 1982) whereas the final conversion of the maghemite to hematite may be a much slower and later process, brought about in the cooling crust as it is carried outwards from the zones of accretion.

Finally, considering the fact that most or all Tertiary basalts in Iceland have undergone the complex mineralogical transformations described here, it seems surprising that the rocks retain their original remanent thermal magnetic directions. That they do so, indeed, has been shown by countless studies, and by the success of paleomagnetism as a stratigraphic tool in Iceland and elsewhere.

Acknowledgements

This research was supported by grants from the Icelandic Science Foundation and the University of Iceland Research fund. The samples were supplied by Dr. Leo Kristjansson of the Science Institute, University of Iceland. Kristjan Jonsson assisted with Mössbauer analyses and Aevar Johannesson with photography and the preparation of the samples. The probe analyses were done at the Industrial Research Inst., Iceland, (EDX) and the Nordic Volcanol. Inst. (WDX), University of Iceland. N. Oskarsson assisted with the X-ray diffraction analysis and contributed to the paper in various ways.

References

Ade-Hall, J. M., Palmer, H. C., and Hubbard, T. P. (1971) The magnetic and opaque petrological response of basalts to regional hydrothermal alteration. *Geophys. J. astron Soc.*, **24**, 137–74.

Akimoto, S. and Kushiro, I. (1960) Natural occurrence of titanomaghemite and its relevance to the unstable magnetisation of rocks. *J. Geomagn. Geoelect.*, **11**, 94–110.

Allan, J. E. M., Coey, J. M. D., Rosende, M. and Fabris, J. D. (1988) Magnetic properties of iron-rich oxysoils. *Phys. Chem. Mineral.*, **15**, 470–5.

——— Sanders, I. S., Schwertmann, U., Friedrich, G., and Wiechowski, A. (1989) An occurrence of a fully-oxidised natural titanomaghemite in basalt. *Mineral. Mag.*, **53**, 299–304.

Aragon, R. and Honig, J. M. (1988) Mean-field model of the Verwey transition in magnetite. *Phys. Rev.*, **B37**, 209–18.

Basta, E. Z. (1960) Natural and synthetic titanomagnetites (the system Fe_3O_4-Fe_2TiO_4-$FeTiO_3$). *Neues Jahrb. Mineral. Abh.*, **94**, 1017–48.

Becker, H. (1980) Magnetic anomalies (DZ) in NE-Iceland and their interpretation based on rock-magnetic investigations. *J. Geophys.*, **47**, 43–56.

Carmichael, C. M. (1961) The magnetic properties of ilminite-hematite crystals. *Proc. Roy. Soc. London, Ser. A*, **263**, 508–30.

Carmichael, I. S. E. (1967) The iron-titanium oxides of salic volcanic rocks and their associated ferromagnesian silicates, *Contrib. Mineral. Petrol.*, **14**, 36–64.

Elmore, W. C. (1938) Ferromagnetic colloid for studying magnetic structures. *Phys. Rev.*, **54**, 309–10.

Fridleifsson, I. B. and Kristjansson, L. (1972) The Stardalur magnetic anomaly, SW-Iceland. *Jökull*, **22**, 69–78.

Haggerty, S. E. (1976) Oxidation of opaque mineral oxides in basalts. In *Reviews in Mineralogy,* **3.** *Oxide Minerals.* (Rumble, III, D., ed.). Mineralogical Society of America, Hg-1–Hg-98.

——and Baker, I. (1967) The alteration of olivine in basaltic and associated lavas. Part 1: High temperature alteration. *Contrib. Mineral. Petrol.,* **16,** 233–57.

Häggström, L., Annersten, H., Ericsson, T., Wäppling, R., Karner, W., and Bjarman, S. (1978) Magnetic dipolar and electric quadrupolar effect on the Mössbauer spectra of magnetite above the Verwey transition. *Hyperf. Int.,* **5,** 201–14.

Helgason, Ö, Steinthorsson, S., Madsen, M. B., and Mørup, S. (1990) On anomalously magnetic basalt lavas from Stardalur, Iceland. Ibid., **57,** 2209–14.

——Gunnlaugsson, H. P., Steinthorsson, S., and Mørup, S. (1992) High temperature stability of maghemite in partially oxidised basalt lava. Ibid. (in press).

Imsland, P. (1984) *Petrology, Mineralogy and Evolution of the Jan Mayen Magma System.* Soc. Sci. Isl., Reykjavík, 332 pp.

Irving, E. (1970) The mid-Atlantic ridge at 45°N, XVI. Oxidation and magnetic properties of basalt. Review and discussion. *Can. J. Earth Sci.,* **7,** 1528–38.

Kristjansson, L. (1985) Magnetic and thermal effects of dike intrusions in Iceland—locations and paleomagnetic characteristics of samples. *J. Geophys. Res.,* **90,** 10129–35.

Jensen, A. (1968) Opaque minerals in the Precambrian plutonic rocks of Bornholm and their relation to the development of these rocks. *Medd. Dansk. Geol. Foren.,* **18,** 79–96.

Levi, S., Audunsson, H., Duncan, R. A. Kristjansson, L., Grillot, P. V., and Jakobsson, S. P. (1990) Late Pleistocene geomagnetic excursion in Icelandic lavas: Confirmation of the Laschamp excursion. *Earth Planet. Sci., Letters,* **96,** 443–57.

Lindsley, D. H. (1976*a*) The crystal chemistry and structure of oxide minerals as exemplified by the Fe-Ti oxides. In *Reviews in Mineralogy,* **3.** *Oxide Minerals.* (Rumble, III, D., ed.). Mineralogical Society of America, L-1–L-60.

——(1976*b*) Experimental studies of oxide minerals. In *Reviews in Mineralogy,* **3.** *Oxide Minerals.* (Rumble, III, D., ed.). Mineralogy Society of America, L-61–L-88.

Madsen, M. B., Mørup, S., and Knudsen, J. M. (1989) Extraterrestrial magnetite studied by Mössbauer spectroscopy. *Hyperf. Int.,* **50,** 659–66.

Mørup, S., Saksager, O., Madsen, M. B., Bentzon, M. D. and Koch, C. J. W. (1990) Weathering of basalt in an arctic climate. Ibid., **57,** 2269–74.

O'Reilly, W. (1984) *Rock and Mineral Magnetism.* Chapman and Hall, New York, 220 pp.

Oskarsson, N., Sigvaldason, G. E., and Steinthorsson, S. (1982) A dynamic model of rift zone petrogenesis and the regional petrology of Iceland. *J. Petrol.,* **23,** 28–74.

Ramdani, A., Steinmetz, J., Gleitzer, C., Coey, J. M. D., Friedt, J. M. (1987) Pertubation de l'echange electronique rapide par les lacunes cationiques dans $\mathrm{Fe}_{3-x}\mathrm{O}_4$ ($x \leq 0.09$). *J. Phys. Chem. Solids,* **48,** 217–28.

Ramdohr, P. (1953) Ulvöspinel and its significance in titaniferous iron ores. *Econ. Geol.,* **48,** 677–88.

Readman, P. W. and O'Reilly, W. (1972) Magnetic properties of oxidised (cation-deficient) titanomagnetites $(\mathrm{Fe, Ti}, \square)_3\mathrm{O}_4$. *Geomag. Geoelect.,* **24,** 69–90.

Rumble, D. (1976) Oxide minerals in metamorphic rocks. In *Reviews in Mineralogy, Oxide Minerals.* (Rumble, III, D., ed.). Mineralogical Society of America, R-1–R-24.

Sato, M. and Wright, T. L. (1966) Oxygen fugacities directly measured in magmatic gases. *Science,* **153,** 1103–5.

Smith, B. M. (1987) Consequences of the maghemitisation on the magnetic properties of submarine basalts: Synthesis of previous works and results concerning basement rocks from mainly D.S.D.P. Legs. 51 and 52. *Phys. Earth Planet. Int.,* **46,** 206–26.

Steinthorsson S. and Sigvaldason, G. E. (1971) *Report on petrological investigations at Stardalur* (in Icelandic). Sci. Inst., University of Iceland (Mimeographed).

——Kristjansson, L., and Sigvaldason, G. E. (1971) Studies of drill cores from an unusual magnetic high in SW-Iceland. (Abstr.). *1st Eur. Earth Planet. Phys. Colloq.,* Reading, England.

——Oskarsson, N., Arnorsson, S., and Gunlaugsson, E. (1987) In *Chemical Transport in Metasomatic Processes.* (Helgeson, H. C., ed.). D. Reidel Publ. Co., 355–87.

Tanaka, H. and Kono, M. (1987) Mössbauer spectra on titanomagnetite: A reappraisal. *J. Geomag. Geoelectr.,* **39,** 463–75.

Walker, G. P. L. (1960) Zeolite zones and dike distributions in relation to the structure of the basalts of eastern Iceland. *J. Geol.,* **68,** 515–28.

Watkins, N. D. and Haggerty, S. E. (1967) Primary oxidation and petrogenesis in a single lava. *Contrib. Mineral. Petrol.,* **15,** 251–71.

[*Manuscript received 23 December 1990:*
revised 10 November 1991]

Appendix: Descriptions of samples

HV10 Late-glacial picritic basalt, Austara Hraunssels-Vatnsfell, Reykjanes Peninsula, SW Iceland: Primary oxide phases are $\mathrm{Im_{SS}}$, $\mathrm{Mt_{SS}}$ and chrome spinel. Individual crystals are rather small, and $\mathrm{Im_{SS}}$ greatly exceeds $\mathrm{Mt_{SS}}$ in volume. Chrome spinel occurs both included in olivine and in the groundmass, usually zoned to titanomagnetite. The sample is irregularly oxidised, with patches showing extreme oxidation with meta-ilmenite and hematite exsolution in the silicates. Very limited oxyexsolution is seen in the $\mathrm{Mt_{SS}}$ (stages C1 and C2) which however appears heterogeneously magnetic under the magnetite colloid. Only in this sample did XRD-measurements of the magnetic fraction reveal variation in composition: the spinel appeared zoned from $\mathrm{Mt_{100}}$ to $\mathrm{Mt_{72}}$ and the rhombohedral phase gave a peak corresponding to almost pure ilmenite and another corresponding to ilmenohematite ($\mathrm{Im_{20}Hm_{80}}$).

NU12-1 Pleistocene alkali basalt, Núpakotsnúpur, Eyjafjöll, S. Iceland: small grains of primary Im$_{\mathrm{SS}}$ and Mt$_{\mathrm{SS}}$ evenly distributed throughout the sample. Generally stage C3, but in places higher degree of oxidation where the Mt$_{\mathrm{SS}}$ has altered to Hm + Pb (stage C7) and Hm is exsolved from silicates.

LX-2 and *LX-6*, Lokufjall Mt, Hvalfjordur, W. Iceland. Boths samples are from the same Plio-Pleistocene tholeiite lava flow, 14 and 25 cm from a 1.3 m thick dyke, respectively. Despite this, their mineralogy and oxidation state are quite different, with *LX-6* being more oxidised and containing more primary Im$_{\mathrm{SS}}$. Different rates of crystallisation owing to different distance to the surface of the lava flow may account for this. *LX-2* contains a relatively large quantity of rather fine grained oxide phase, which is almost exclusively unexsolved Mt$_{\mathrm{SS}}$ (stage C1), as indicated by the magnetic colloid. The anisotropic nature of the grains, however, belies the presence of submicroscopic ilmenite intergrowths. The sample contains hardly any primary Im$_{\mathrm{SS}}$. In *LX-6* primary Mt$_{\mathrm{SS}}$ and Im$_{\mathrm{SS}}$ in approximately equal proportions. Oxidation is uneven; in parts of the sample stage C3, in other parts stage C7 (Mt$_{\mathrm{SS}}$ altered to Pb + Hm) and much internal reflection indicates Hm-exsolution in silicates. Only in this sample is there evidence in the Mössbauer spectrum of two magnetite phases, one pure and the other with 8% ulvöspinel.

LY-7 Plio-Pleistocene olivine basalt, Lokufjall Mt, Hvalfjordur (N side): the rock is rather coarse grained, containing primary lath-shaped Im$_{\mathrm{SS}}$ crystals and Mt$_{\mathrm{SS}}$ of two generations, largish equant crystals and smaller skeletal ones. Limited amount of octahedral lamellae in Mt$_{\mathrm{SS}}$ (stage C3) but pronounced red internal reflection attesting to hematite exsolution in silicates. Some of the skeletal magnetite completely altered to non-magnetic hematite. Mobility of iron in the rock during alteration manifest by cavities lined with concentric rings of Hm and Mt.

WJC-6 Plio-Pleistocene olivine basalt, Blikdalsá, Kjalarnes near Reykjavik: rather coarse grained. Large laths of Im$_{\mathrm{SS}}$ predominate. Mt$_{\mathrm{SS}}$ in two generations, equant and skeletal, is magnetically homogeneous, stage C1. According to the Mössbauer study this sample contains the highest proportion of maghemite in the magnetic phase, and under the microscope maghemite is seen both replacing entire grains and parts of crystals (Fig. 4*c*).

JGC-7 Tertiary feldspar-porphyritic basalt, Njörvadalsá, Reydarfjordur, E. Iceland; contains large laths of Im$_{\mathrm{SS}}$, and equant crystals of Mt$_{\mathrm{SS}}$ exhibiting very limited oxyexsolution (C1–C2 stage). No hematite is visible, either in oxides or silicates, but in some spinel grains small oriented white specks are seen, incipient oxidation to maghemite.

OGC-1 Tertiary tholeiite. Red internal reflection attests to hematite exsolution in silicates. Oxyexsolution in equant grains of Mt$_{\mathrm{SS}}$ generally fairly limited (stage C2 to C3), but in places the Mt$_{\mathrm{SS}}$ is replaced partly or wholly by Hm + Pb (stage C7), and the Im$_{\mathrm{SS}}$ gone to hemoilmenite.